Climate Dynamics manuscript No.
(will be inserted by the editor)

Shortwave and longwave radiative contributions to global energy imbalance under increasing CO_2

Angeline G. Pendergrass · **Aaron Donohoe** · **Kyle C. Armour**

Received: May 2012 / Accepted: August 2014

Abstract Greenhouse gas forcing is primarily in the longwave (LW), but the transient disequilibrium response at the top of the atmosphere (TOA) to a CO_2 ramp forcing is primarily in the shortwave (SW). Here we establish that this is because the temperature rapidly response tot he greenhouse forcing, resulting in a Plank feedback that nearly balances the LW forcing, and so remaining imbalances manifest themselves in the shortwave. Furthermore, we show that the SW feedbacks are responsible for most of the intermodel spread in transient TOA disequilibirum using a model of the global-mean TOA radiation using only the forcing, SW and LW feedbacks, and an effective heat capacity.

Keywords climate change · global energy budget · transient climate forcing

1 Introduction

Global conservation of energy is a powerful tool for understanding Earth's climate and climate changes. Variations in atmospheric composition that result in a net positive energy imbalance at the top-of-atmosphere (TOA) cause the Earth to warm, with the world ocean as the primary reservoir for excess energy [Levitus et al(2001)Levitus, Antonov, Wang, Delworth, Dixon, and Broccoli, Hansen et al(2005)Hansen, Nazarenko, Ruedy, Sato, Willis, Del Genio, Koch, Lacis, Lo, Menon, Novakov, Perlwitz, Russell, Tausnev, Thresher, and Yao, Church et al(2011)Church, White, Gregory, Lambeck, Milne, Stammer, Unnikrishnan, and Velicogna]. In turn, increasing global surface temperature increases emission of longwave (LW) radiation to space (via the Planck feedback) until the global average LW emission once again balances the net shortwave (SW) radiation at the TOA. A schematic of the response of the Earth's energy budget to a step change in greenhouse gas concentrations is shown in Fig. 1 A. Longwave emission is initially reduced, but returns

A. G. Pendergrass
University of Washington
Department of Atmospheric Sciences
Box 351640
E-mail: angie@atmos.washington.edu

S. Author
second address

toward its original value as the climate warms; over several millennia, energy balance is restored and climate is stabilized. In this canonical view of the climate response to greenhouse gas forcing, the energy accumulation within the climate system (i.e. the shaded red area in Fig. 1A) is a consequence of decreased LW emission due to enhanced greenhouse gas levels.

Is reduced LW emission from anthropogenic greenhouse gases the primary driver of the Earth's present energy imbalance (e.g., [Hansen et al(2005)Hansen, Nazarenko, Ruedy, Sato, Willis, Del Genio, Koch, Lacis, L
Since greenhouse gas levels and global temperature change with time, a description of climate adjustment to sustained forcing changes (i.e. Fig. 1A) is of little use. Moreover, forcing agents that are radiatively active in the SW (e.g., light-scattering aerosols) as well as SW climate feedbacks (e.g., cloud and ice albedo feedbacks) drive changes in the TOA energy balance through changes in global SW absorption, further complicating the picture. The limited length of satellite TOA radiation measurements precludes determination of the relative contributions of SW absorption and LW emission changes to the global energy imbalance by direct observation. However, global climate model (GCM) simulations afford investigation of the global energy budget under a range of forcing scenarios. Here we make use of the World Climate Research Programme's (WCRP's) Coupled Model Intercomparison Project phase 3 (CMIP3) multi-model dataset [Meehl et al(2007)Meehl, Covey, Taylor, Delworth, Stouffer, Latif, McAvaney, and Mitchell] (see Section 3).

[Trenberth and Fasullo(2009)] consider the CMIP3 multi-model mean response to the SRES A1B forcing scenario, which includes realistic projections for future greenhouse gas and aerosol levels. They report the somewhat surprising result that TOA LW emission changes little over time, so that global energy imbalance is driven almost entirely by SW absorption. Figure 1C shows this result under an idealized 1% per year to CO_2 doubling forcing scenario (CO_2 forcing is increased approximately linearly in time for 70 years). In the multi-model mean the energy available to heat the Earth comes from increased SW absorption, which is at odds with the canonical picture of climate adjustment to greenhouse gas forcing (c.f. Fig. 1A and Fig. 1C). However, models simulate a wide range of responses: some show substantial reductions in LW emission under CO_2 ramping while others show substantial increases LW emission under CO_2 ramping.

In order to quantify the relative contributions of SW absorption and LW emission to energy accumulation over the CO_2 ramping period, we define the ratio of integrated anomaly (relative to the global energy balance in the pre-industrial) in SW absorption (SW') to the integrated net TOA imbalance ,

$$R_{SW} = \frac{\int_0^{70} \Delta SW'(t)dt}{\int_0^{70} (\Delta SW(t) - \Delta LW(t))dt}. \quad (1)$$

When global warming is driven primarily by reduced LW emission, as is the case in the canonical response to a greenhouse forcing (see Fig. 1A) all of the energy accumulation is due to perturbations in the LW and $R_{SW} = 0$. If warming is driven primarily by increased SW absorption, as is the case if the solar constant were increased (see Fig. 1B), the energy accumulation is due to perturbations in the SW (the blue shaded area) and is damped by the LW response (the LW increases and the hatched

red shaded area is the energy lost from the system due to the LW perturbation). In this case, the net energy accumulation is the area between the SW and LW curves and is equal to the difference in SW accumulation and the integrated LW increase; $R_{SW} > 1$ because the SW accumulation is greater than the total energy accumulation due the energy lost by the LW perturbation. In the CMIP3 ensemble mean response $R_{SW} \approx 1$ (see Fig. 1C) indicating that, despite the greenhouse forcing ($\approx 4Wm^{-2}$), the LW radiation is nearly unchanged over the ramping period while the SW absorption increases and is responsible for the energy accumulation in the climate system. This result runs contrary to the canonical behavior expected from a greenhouse forcing experiment.

The CMIP3 models simulate R_{SW} values ranging from 0.026 to 2.9 (Table 1). This wide spread, under the same CO_2 forcing (at least approximately), suggests a range of possible climate response to transient greenhouse gas forcing. To isolate the fundamental mechanisms responsible for the mean model response and spread across the models, we focus our analysis on the idealized 1% per year to CO_2 doubling experiment and do not address here variation in global energy budgets under more realistic, and complex, forcing scenarios.

We first describe in greater detail our use of the CMIP3 archive and methods of analysis. We then develop an energy balance model based on linear climate feedbacks that we use to interpret the GCM simulations. We show that the ensemble mean and individual model responses arise from relatively simple considerations of the forcing, planetary heat capacity, and linear LW and SW feedbacks. The difference in temporal evolution of SW absorption and LW emission across the CMIP3 GCMs, and thus the relative contributions of SW and LW changes to net heating (R_{SW}), can be explained primarily by variations net SW feedback across the models. Variations in net LW feedbacks across the models play a negligible role in the partitioning of TOA response between SW absorption and LW emission.

2 Data: GCM CO_2 ramping experiments

Data were downloaded from the World Climate Research Programme's (WCRP's) Coupled Model Intercomparison Project phase 3 (CMIP3) multi-model dataset [Meehl et al(2007)Meehl, Covey, Taylor, Delworth, S for the 1% per year to CO_2 doubling (`1pctto2x`) scenario. We show calculations for `run1` of each model; additional ensemble members for models where they are available behave similarly to `run1` Variables include surface air temperature, upwelling and downwelling LW and SW radiation at the TOA for these models where all of these data are available.

Timeseries of global, annual mean data are smoothed with a three passes of a 1-2-1 filter [Gonzalez and Woods(2002)]. The differences are taken from first datapoint of the smoothed timeseries, which is a weighted average of the first seven years of the ramping, to ensure consistency of datasets. We consider the change in SW absorption and OLR from the beginning of the experiment; this excludes any initial imbalance in the models. The difference between absorbed SW and OLR is typically less than 2 W m^{-2} but as big as 6 W m^{-2} in one model. Some models have changes in down-

welling SW radiation which are less than 0.5 W m^{-2} . We avoided these by only using changes in net SW absorption in our calculations.

3 Method: Linear feedback model

At any time t, the energy imbalance N at the TOA is the difference between radiative forcing Q and a linear feedback r times the temperature difference from the beginning of the ramping ΔT,

$$N(t) = Q(t) - r\Delta T(t). \tag{2}$$

Both Q and r have LW and SW components. The formula in [Forster and Taylor(2006)] is used in all calculations here.

As in [Forster and Taylor(2006)], we calculated the feedbacks r_{SW} and r_{LW} by regressing the N_{SW} and N_{LW} on ΔT. These are shown in Table 1 Because we calculate these feedbacks for the CO_2 ramping rather than instantaneous doubling, the intercept is zero and we do not distinguish between fast and slow feedbacks.

To relate the TOA energy imbalance to the transient heating, we calculate an effective heat capacity h of the climate system,

$$h(t) = \frac{\int_0^t N(t)dt}{\Delta T(t)}. \tag{3}$$

We use the integral rather than the differential form of the heating equation because the temperature change is more stable when calculated relative to the beginning of the experiment rather than locally. We calculate the effective heat capacity from the ensemble mean integrated energy imbalance and surface temperature change, shown in Fig. 3. The heat capacity increases with time because as the forcing is applied for longer, ocean mixing allows an increasing depth of ocean to warm; the land also heats to increasing depths but this a much smaller factor.

These equations can be solved iteratively for temperature,

$$\Delta T(t) = \frac{\Sigma_{t=1}^{t} Q - r\Sigma_{t=1}^{t-1}\Delta T}{h(t)}, \tag{4}$$

to make a simple model of the SW and LW energy imbalances,

$$\Delta SW_a = Q_{SW} - r_{SW}\Delta T, \tag{5}$$

$$\Delta OLR = -(Q_{LW} - r_{LW}\Delta T). \tag{6}$$

We use the feedbacks calculated for each GCM in this model to calculate time-series of LW and SW at the TOA where the only intermodel differences are due to the LW and SW feedbacks (Fig. 4). We quantify the error of this model for each curve by calculating the mean absolute error over the last ten years of the ramping (Fig. 5).

4 Linear feedback model experiments

In GCMs, the LW feedback is negative (damping any forcing), while the sign of the SW feedback is negative in some models and positive in others. The energy absorbed by the planetary energy budget is thus controlled more by the variations in SW feedback than in LW feedback. To show that the magnitude of the feedback strongly controls the TOA SW and LW curves, we run our linear feedback model with a variety of driving feedbacks. First, we use the LW and SW feedbacks calculated by regressing each GCM separately. Second, we use each individual GCM's SW feedback, but the ensemble mean LW feedback. Third, we use the individual SW feedbacks but ensemble mean SW feedback. Finally, we use both ensemble mean LW and SW feedbacks (no variation across GCMs).

The mean absolute of the LW and SW curves for these four experiments is shown in Fig. 5. The models are shown in order of increasing SW feedback. Errors are lowest when individual SW and LW feedback values are used; they are only slightly higher when the same LW feedback is used for each model (and GCMs still have their own SW feedback). In contrast, using the same SW feedback and different LW feedbacks results in much greater error, which increases with the difference of the GCM SW feedback from the ensemble mean. Using both ensemble mean LW and SW feedbacks is comparable to using the ensemble mean LW feedback. Furthermore, this pattern is the same for LW and SW curves. That is, in order to get the correct OLR curve, it is more important to have the correct SW feedback than LW feedback. These experiments highlight the importance of the SW feedback in determining the transient TOA radiative disequilibrium response to greenhouse gas (LW) forcing.

From the linear feedback model, we calculate what F_{SW} is for a range of SW and LW feedbacks (Fig. 6). The contours of F_{SW} are nearly flat, indicating that over the range of LW feedback seen in GCMs, the LW feedback has little effect on how much the disequilibrium is in the SW or LW. Instead, the magnitude of F_{SW} is strongly controlled by the SW feedback. For small SW feedback, the disequilibrium in the SW (and thus F_{SW}) is small. As the SW feedback becomes larger (more negative here), F_{SW} increases. For a SW feedback of about 0.7, F_{SW} is one. For larger values of the SW feedback, it continues to increase. It is relevant here that the SW forcing of CO_2 is small (though we do include it).

Also shown in Fig. 6 are dots showing the LW and SW feedbacks and the value of F_{SW} for the GCMs. The qualitatively match the simple model findings. While the range of SW and LW feedbacks across models is comparable (around 2 W m^{-2} K^{-1}), the SW feedback controls whether the disequillibrium is in the LW or SW.

5 Summary and discussion

Here we have considered why the TOA radiative disequilibrium to a greenhouse gas ramp is primarily in the SW rather than the LW in CMIP3 GCM experiments. We find that this is driven primarily by the SW feedback, and that the range of the LW feedback in the CMIP3 models has little effect on the SW and LW contributions to radiative disequilibrium (i.e., the contour lines in Fig. 6 are nearly horizontal).

Table 1 LW and SW feedbacks and ratio of SW to net TOA integrated imbalance (F_{SW}) for each GCM.

Model	r_{SW}	r_{LW}	R_{SW}
IPSL CM4	-1.9	2.8	2.3
MIROC3 2 HIRES	-1.7	2.5	2.9
CNRM CM3	-1.5	3.2	2
MIROC3 2 MEDRES	-1.5	2.4	1.5
CCCMA CGCM3 1	-1.3	2.6	2.1
CSIRO MK3 5	-1.3	2.5	1.6
CSIRO MK3 0	-1.2	2.8	1
UKMO HADGEM1	-0.97	2.2	1.2
UKMO HADCM3	-0.93	2	1.3
MPI ECHAM5	-0.9	1.9	1.6
MRI CGCM2 3 2A	-0.72	2.1	1.3
GFDL CM2 0	-0.63	2.3	0.68
GISS MODEL E H	-0.57	1.8	0.51
NCAR CCSM3 0	-0.49	2.2	0.58
GFDL CM2 1	-0.33	2	1.1
INMCM3 0	-0.19	1.9	0.026
NCAR PCM1	-0.15	2.1	-0.21
MIUB ECHO G	0.0002	1.5	0.51
IAP FGOALS1 0 G	0.33	2.3	-0.54

The TOA radiative disequilibrium is the rate of energy accumulation by the planet. It is related to the rate of surface temperature change via the heat capacity (as in Eqn. 3). To the extent that the heat capacity is independent of the feedback strength (it mostly is), this implies that surface temperature change is controlled by the SW feedback strength, rather than the LW.

If SW feedbacks are so important, what controls them? [Trenberth and Fasullo(2009)] also start with the idea that absorbed SW controls the TOA disequilibrium, and they argue that this implies that changes in cloud fraction control transient climate change. While we do not disagree that clouds are important, there are other factors as well. The SW water vapor feedback composes about one-third of the SW feedback in the ensemble mean (EVIDENCE, AND HOW MUCH OF INTERMODEL SPREAD?). Surface albedo changes are also important. The surface albedo contribution to the inter-model spread in SW feedbacks is small compared to that in clouds [Donohoe and Battisti(2011)]. Finally, [Trenberth and Fasullo(2009)] did not take into account the changes in aerosol forcing that are present in the A1b scenario, in particular the decrease in reflecting aerosol from 2030 until the end of the century.

Acknowledgements We acknowledge the modeling groups, the WCRP's Working Group on Coupled Modeling (WGCM) for their roles in making available the WCRP CMIP3 multi-model dataset. Support of this dataset is provided by the Office of Science, U.S. Department of Energy.

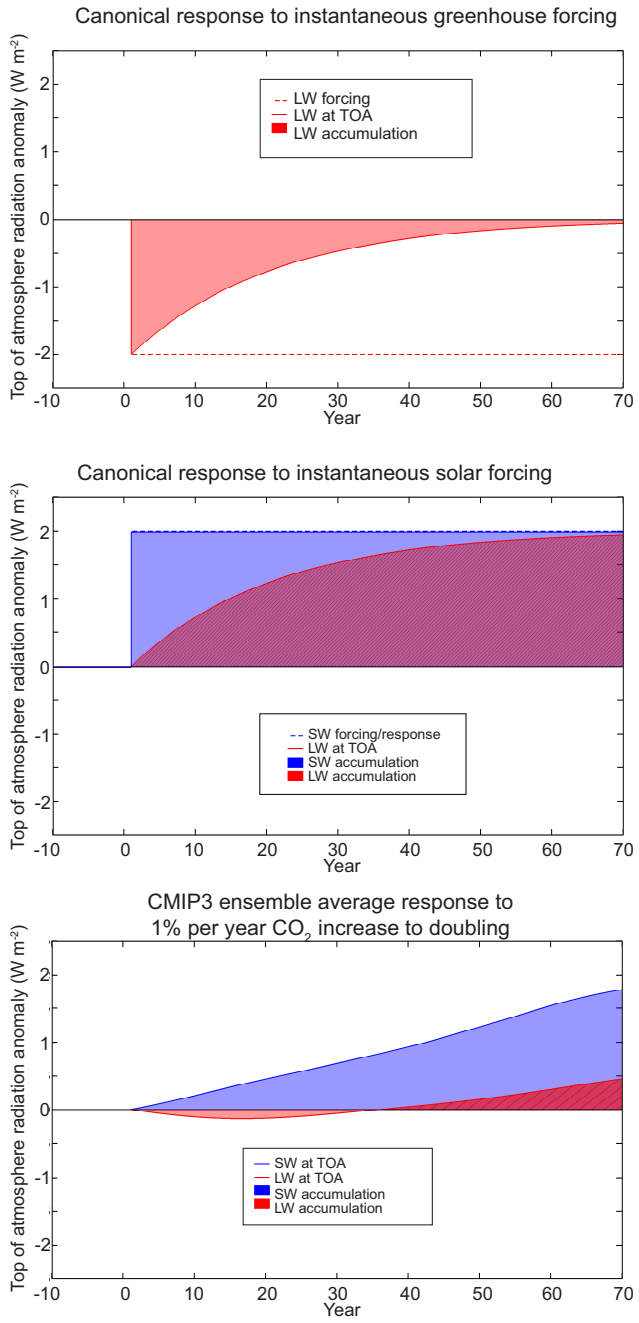

Fig. 1 (A) Idealized response of radiation at the top of atmosphere to an instantaneous greenhouse forcing of 2.5 W m^{-2} assuming a radiative adjustment e-folding time of 20 years. The shaded red area is the longwave energy accumulation. (B) As in (A) but in response to an instantaneous SW increase of 2.5 W m^{-2}. In this case, the net energy accumulation is the difference between the SW energy accumulation (the shaded blue area) and the LW increase (the hatched red area where the hatching indicates that the LW response leads to a cooling of the climate system). The CMIP3 ensemble average radiative response in the 1% CO_2 increase to doubling experiments. The shaded area represent the energy accumulation by SW (blue) and LW (red) anomalies and the hatched red area indicates energy loss by LW processes.

Fig. 2 Global-, ensemble- mean TOA SW, LW, and net radiative imbalance and forcings (from [Forster and Taylor(2006)]) for 1% per year to CO_2 doubling experiment. Radiative imbalance curves are smoothed with three passes of a 1-2-1 filter.

References

[Donohoe and Battisti(2011)] Donohoe A, Battisti DS (2011) Atmospheric and suface contributions to planetary albedo and their relationship to the total meridional energy transport 24:4401–17

[Forster and Taylor(2006)] Forster P, Taylor K (2006) Climate forcings and climate sensitivities diagnosed from coupled climate model integrations. Journal of Climate 19(23):61816194

[Gonzalez and Woods(2002)] Gonzalez RC, Woods RE (2002) Digital Image Processing, 2nd edn. Prentice Hall, Upper Saddle River, N. J.

[Hansen et al(2005)Hansen, Nazarenko, Ruedy, Sato, Willis, Del Genio, Koch, Lacis, Lo, Menon, Novakov, Perlwitz, Russell, Schmidt, and Tausnev] Hansen J, Nazarenko L, Ruedy R, Sato M, Willis J, Del Genio A, Koch D, Lacis A, Lo K, Menon S, Novakov T, Perlwitz J, Russell G, Schmidt GA, Tausnev N (2005) Earth's energy imbalance: Confirmation and implications. Science 308(5727):1431–1435, DOI 10.1126/science.1110252, URL http://www.sciencemag.org.offcampus.lib.washington.edu/content/308/5727/1431

[Levitus et al(2001)Levitus, Antonov, Wang, Delworth, Dixon, and Broccoli] Levitus S, Antonov J, Wang J, Delworth T, Dixon K, Broccoli A (2001) Anthropogenic warming of earth's climate system. Science 292(5515):267

[Meehl et al(2007)Meehl, Covey, Taylor, Delworth, Stouffer, Latif, McAvaney, and Mitchell] Meehl GA, Covey C, Taylor KE, Delworth T, Stouffer RJ, Latif M, McAvaney B, Mitchell JF (2007) THE WCRP CMIP3 multimodel dataset: A new era in climate change research. Bulletin of the American Meteorological Society 88(9):13831394

[Trenberth and Fasullo(2009)] Trenberth KE, Fasullo JT (2009) Global warming due to increasing absorbed solar radiation. Geophysical Research Letters 36(7):L07,706

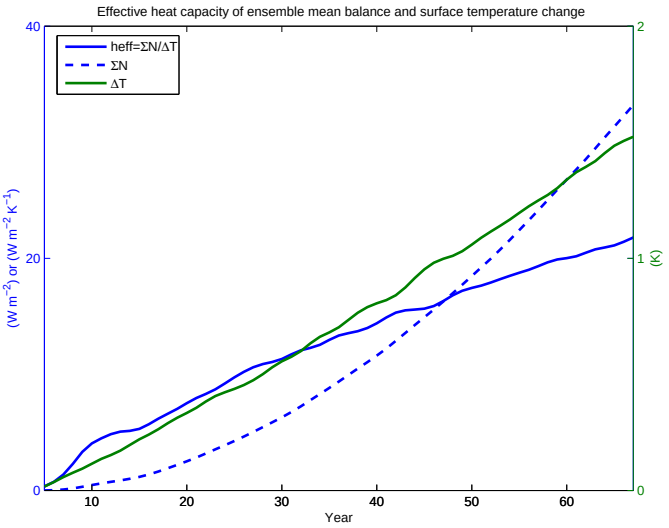

Fig. 3 The heat capacity (time-dependent, ensemble mean, solid blue line) is the ratio of the integrated ensemble-mean TOA energy imbalance to global mean surface temperature change (dashed blue line) and the change in surface temperature relative to the beginning of the ramping (green line, note different *y*-axis). Energy balance and temperature change are smoothed with three passes of a 1-2-1 filter before calculation.

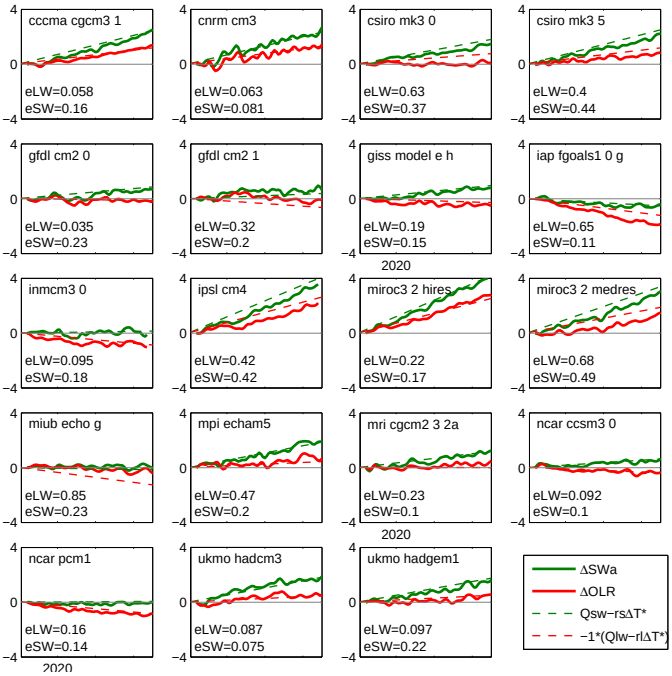

Fig. 4 Timeseries of SW and LW radiation from CMIP3 models (solid lines) and using the linear feedback model of equation 4 (dashed lines). Feedback values are calculated for each model separately; the heat capacity is the same for all models (see Fig. 3). Mean absolute error of the model for the LW and SW curves over the last ten years is shown in each panel.

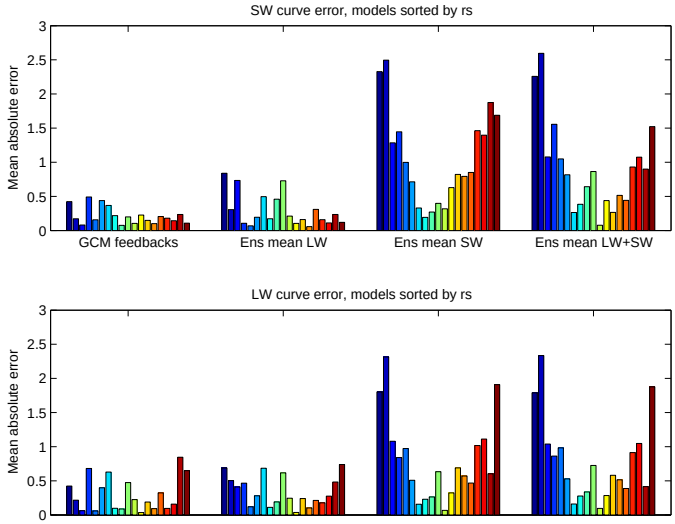

Fig. 5 Mean absolute error of the SW (top) and LW (bottom) curves (shown in Fig. 4) over the last 10 years of ramping of linear feedback model for CMIP3 GCMs. Four different setups for the model are: LW and SW feedbacks calculated individually for each GCM, ensemble mean LW feedback but individual SW feedbacks, ensemble mean SW feedback and individual LW feedbacks, and ensemble mean SW and LW feedbacks. Each bar represents the error for one GCM, and the GCMs are sorted by their SW feedback.

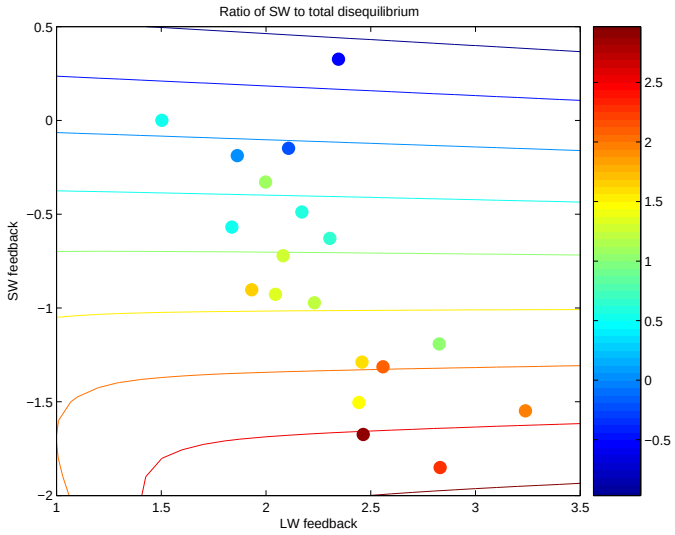

Fig. 6 The fraction of TOA imbalance in the SW at the time of CO_2 doubling for the linear feedback model (contours) as a function of LW and SW feedbacks. Circles show the location of each CMIP3 model in LW- versus SW-feedback space, and the color of the dots shows the fraction of imbalance in the SW.

Fig. 7 3 balls